Journal of Chemistry and Technologies, 2026, *34*(2), 412-424

Journal of Chemistry and Technologies

pISSN 2663-2934 (Print), ISSN 2663-2942 (Online).

journal homepage: http://chemistry.dnu.dp.ua
editorial e-mail: chem.dnu@gmail.com

UDC 664.895:641.82

SYNTHESIS OF ZEOLITES OF THE CHABAZITE GROUP BASED ON NATURAL MINERALS OF NAKHCHIVAN: THE INFLUENCE OF VARIOUS FACTORS ON THE PROCESS OF THEIR CRYSTALLIZATION

Nuray M. Azimova[1], Gunel A. Mamedova[1,2*], Sevda H. Aliyeva[1], Rena H. Jamalova[3], Gulnura M. Mammadova[3], Mushkunaz B. Hasanova[3], Kamala F. Ibrahimova[4], Parvana E. Kalantarova[4], Ramila E. Huseynova[4], Aliye M. Pashayeva[4], Afsana F. Heybatova[4]

[1]*Nakhchivan State University, Nakhchivan, AZ7012, Azerbaijan*
[2]*Institute of Natural Resources, Nakhchivan State University, Nakhchivan, Azerbaijan*
[3]*Azerbaijan State Oil and Industry University, Azerbaijan*
[4]*Institute of Chemistry, Ministry of Science and Education of the Republic of Azerbaijan, Azerbaijan, Baku*
Received 1 December 2025; accepted 13 March 2026; available online 20 June 2026

Abstract

Zeolites of the chabazite group (gmelinite, levyne, and erionite) having practical significance were synthesized on the basis of natural minerals of the Nakhchivan Autonomous Republic in the presence of a structure-directing agent – tetramethylammonium hydroxide. Samples of halloysite from the Pirigol deposit, volcanic glass (obsidian) from the peak of Gapydzhik, and dolomite from the Negram deposit, which were distinguished by phase purity, were used as natural minerals. The influence of temperature, concentration of the thermal solution, and processing time on the crystallization process of gmelinite, levyne, and erionite was studied. It is shown that the hydrothermal synthesis of gmelinite, levyne, and erionite was studied in the temperature range of 100–300 °C, with the concentration of thermal solution NaOH, varying in the range of 10–35 %, for 50–200 hours; 100–300 °C, with the concentration of the NaOH thermal solution varying in the range of 10–35%, for 50–200 hours; 100–300 °C, with a NaOH concentration of 10–35 %, for 50–150 hours; 100–200 °C, with a NaOH concentration of 10–30 %, for 10–20 hours, respectively.

Keywords: gmelinite; levyne; erionite; crystallization; hydrothermal synthesis; chabazite group; zeolite; natural minerals.

СИНТЕЗ ЦЕОЛІТІВ ГРУПИ ШАБАЗИТУ НА ОСНОВІ ПРИРОДНИХ МІНЕРАЛІВ НАХЧИВАНІ: ВПЛИВ РІЗНИХ ФАКТОРІВ НА ПРОЦЕС ЇХ КРИСТАЛІЗАЦІЇ

Нурай М. Азімова[1], Гунель А. Мамедова[1,2], Севда Х. Алієва[1], Рена Х. Джамалова[3], Гульнура М. Маммадова[3], Мушкуназ Б. Гасанова[3], Камала Ф. Ібрагімова[4], Парвана Е. Калантарова[4], Раміла Е. Гусейнова[4], Аліє М. Пашаєва[4], Афсана Ф. Хейбатова[4]

[1]*Нахчиванський державний університет, Нахчиван, AZ7012, Азербайджан*
[2]*Інститут природних ресурсів, Нахчиванський державний університет, Нахчиван, Азербайджан*
[3]*Азербайджанський державний нафтогазовий університет, Азербайджан*
[4]*Інститут хімії, Міністерство науки та освіти Азербайджанської Республіки, Азербайджан, Баку*

Анотація

На основі природних мінералів Нахчиванської Автономної Республіки в присутності агента, що визначає структуру – гідроксиду тетраметиламонію – були синтезовані цеоліти групи шабазиту (гмелініт, левін та еріоніт), які мають практичне значення. Як природні мінерали використовували зразки галлоїзиту з родовища Пірігол, вулканічного скла (обсидіану) з вершини Гапиджик та доломіту з родовища Неграм, які відрізнялися фазовою чистотою. Досліджений вплив температури, концентрації термального розчину та часу обробки на процес кристалізації гмелініту, левіну та еріоніту. Показано, що гідротермальний синтез гмелініту, левіну та еріоніту досліджували в діапазоні температур 100–300 °C за концентрації термального розчину NaOH, що варіювалася в діапазоні 10–35 %, протягом 50–200 годин; 100–300 °C, за концентрації термального розчину NaOH, що варіювалася в діапазоні 10–35 %, протягом 50–200 годин; 100–300 °C, за концентрації NaOH 10–35 %, протягом 50–150 год; 100–200 °C, за концентрації NaOH 10–30 %, протягом 10–20 год відповідно.

Ключові слова: гмелініт; левін; еріоніт; кристалізація; гідротермальний синтез; група шабазиту; цеоліт; природні мінерали.

**Corresponding author: e-mail: sevda.eliyeva@ndu.edu.az*

doi: 10.15421/jchemtech.v34i2.345095

Journal of Chemistry and Technologies, 2026, *34*(2), 412-424

Introduction

Although over 200 zeolites are known and new hypothetical structures are continually being introduced into the scientific arena, the synthesis of some known structures still poses a significant challenge, as they depend on complex reaction procedures, lengthy crystallization, and the use of expensive reagents [1].

Zeolites of the chabazite group are practically important minerals with a wide range of applications, from adsorbents to catalysts [2; 3].

The double six-ring (D6R) structure of gmelinite exhibits a three-dimensional multiporous system with large 12-membered and small 8-membered ring channels [4; 5].

Like other large-pore zeolites, gmelinite is applicable in selective catalysis and gas separation [6; 7], and shows promise as a potential adsorbent for reducing fluoride content in water [8; 9], as well as an adsorbent for alcohols [10].

Levyne is a poorly studied zeolite with a two-dimensional 8-membered ring (8MR) channel system, where single six-membered rings (6MR) of tetrahedra are arranged along the c-axis, forming a cavity and double six-membered rings (D6R) [11; 12]. Two parallel eight-membered channels are interconnected, and extra-framework cations are distributed along the three-fold axis [13].

Zeolite levyne has high practical significance, demonstrating efficiency as an adsorbent for CO_2 [14] and propylene [15], as well as high activity and selectivity in reactions converting methanol to olefins [16] and in the synthesis of methylamines [17; 18].

Erionite, which is constructed from a cancrinite cage and a double hexagonal ring (D6R) [19–21], has recently attracted considerable attention due to its potential application in the selective catalytic reduction of NO_x [22] and in water purification from Cd^{2+}, Cu^{2+}, and Pb^{2+} ions [23].

The study of zeolite crystallization processes based on natural minerals is distinguished by the low cost of the process and the abundance of the original minerals in nature.

Considering the practical importance of chabazite-group zeolites, we aimed to synthesize them using Nakhchivan's mineral resources under more moderate conditions, with 100 % crystallinity and phase purity.

Therefore, this research study examines the technology for synthesizing phase-pure chabazite-group zeolites with 100 % crystallinity using Nakhchivan's mineral resources in the presence of TMAOH. This study investigates the influence of temperature, thermal alkali solution concentration, and process duration on the rate and selectivity of synthesis, and also identifies optimal conditions for producing these zeolites.

Experimental

Local minerals used in the study included halloysite from the Pirigel deposit, dolomite from the Negram deposit, and obsidian from the Gapydzhik peak in the Ordubad district.

Hydrothermal synthesis was conducted in Morey-type autoclaves made of 45MNFT stainless steel with a volume of 18 cm^3 and a filling factor F = 0.8. Hydrothermal crystallization was performed without creating a temperature gradient ($\Delta T = 0$) and without stirring the reaction mixture, in the presence of tetramethylammonium hydroxide (TMAOH). The structure-directing agent (TMAOH) was used in an amount of 5 wt.% of the total initial mass. The volume ratio of the solid to liquid phases was 1 : 5. NaOH solutions of varying concentrations were used as the thermal solution. The mass ratio of the starting components – halloysite (H), dolomite (D), and obsidian (O) – was H : D : O = 1 : 1 : 1.

Hydrothermal synthesis of gmelinite, levyne, and erionite was studied in the temperature range of 100–300 °C, with the concentration of the thermal NaOH solution varying in the range of 10–35 % for 50–200 hours; 100–300 °C, with the concentration of the thermal NaOH solution varying in the range of 10–35 % for 50–150 hours; and 100–200 °C, with the concentration of the thermal NaOH solution varying in the range of 10–30 % for 10–20 hours, respectively.

The optimal ranges of conditions for the synthesis of gmelinite, levyne, and erionite zeolites with 100 % crystallinity and phase purity turned out to be: temperature 200 °C, concentration of thermal NaOH solution (C_{NaOH}) – 20–30 %, processing time – 100 hours; 200 °C, C_{NaOH} – 20–30 %, processing time – 100 hours; and 150 °C, C_{NaOH} – 15–20 %, processing time – 12 hours, respectively.

Identification of zeolite phases was performed using X-ray diffraction (XRD), elemental analysis, thermal analysis (TG/DSC), IR spectroscopy, and scanning electron microscopy (SEM). A Bruker D2 PHASER X-ray diffractometer (CuKα, 2θ = 20–80°) was used in the experiments. IR spectroscopy studies were performed on a Nicolet iS10 FTIR spectrometer in the frequency range of 400–5000 cm^{-1}. Zeolite samples were prepared by pelletizing with KBr in air at a ratio of 1 mg of zeolite to 400 mg of KBr using a PIKE Technologies

Journal of Chemistry and Technologies, 2026, *34*(2), 412-424

hydraulic hand press. The resulting powder was pressed into tablets with a diameter of 1 mm. Thermal studies were conducted on a NETZSCH STA 449 F3 Jupiter thermal analyzer in dynamic mode at temperatures ranging from 20 to 1000 °C.

Elemental analysis was performed using an Oxford Instruments Triton XL system.

Scanning electron microscopy (SEM) was performed on a Hitachi TM3000 table-top microscope 30,000×magnification). The low-vacuum mode allowed for sample analysis without conductive coating deposition.

The degree of crystallinity was calculated based on IR absorption curves. To determine the degree of crystallinity of the zeolite, the irradiation flux intensity was measured proportionally to the maximum transmittance of the zeolite sample in the range of 400–1200 cm^{-1}. This means that the irradiation intensity was measured proportionally to the minimum transmittance of the sample, and the optical density D was determined. The optical density was calculated using the following formula [24]:

$$D = \lg T_{max} - \lg T_{min},$$

where D is the optical density;

T_{max} is the percentage transmittance at the maximum transmittance of the analytical band, and

T_{min} is the percentage transmittance at the minimum transmittance of the analytical band.

The calculated crystallinity data obtained from the IR spectra were also confirmed by X-ray diffraction analysis. The crystallinity of the samples was calculated from the relative peak intensities. According to the ASTM standard, the percentage of crystallinity is determined by the formula [25]:

$$\text{Relative crystallinity (\%)} = \frac{\text{total peak intensity of sample}}{\text{total peak intensity of standard}} 100\ \%.$$

Discussion of results

Zeolites of the chabazite group (gmelinite, levyne, and erionite) were synthesized using Nakhchivan's natural minerals: obsidian, clay, and dolomite. Local halloysite clay was used in the studies. Samples were collected from the Pirigol deposit as the starting material. Halloysite from the Pirigol deposit is characterized by relatively high phase purity. Obsidian from the Gapydzhik peak in the Ordubad district and dolomite from the Negram deposit were used as the starting components.

The chemical compositions of the starting components are presented in Table 1.

Table 1

Chemical compositions of obsidian samples (O) from the Gapydzhik peak of the Ordubad region, halloysite (H) from the Pirigol deposit, and dolomite (D) from the Negram deposit

Element	Weight (%)			Atomic (%)			Amount of oxides (%)			Formula
	O	H	D	O	H	D	O	H	D	
Si	41.58	29.37	3.93	30.75	20.48	2.88	74.97	44.52	7.43	SiO_2
Al	10.52	20.54	-	5.43	12.89	-	12.85	32.78	-	Al_2O_3
Ca	0.63	1.17	26.38	0.43	1.08	20.78	0.77	2.33	31.34	CaO
Na	2.17	0.63	0.77	1.63	0.52	0.42	3.48	0.78	0.93	Na_2O
K	3.01	0.79	0.65	2.08	0.59	0.54	4.96	0.93	0.82	K_2O
Mg	0.49	2.23	17.43	0.31	1.75	13.25	0.65	3.15	23.44	MgO
Fe (III)	0.61	0.98	-	0.49	0.47	-	0.79	1.47	-	Fe_2O_3
Fe (II)	0.32	0.73	0.98	0.17	0.34	0.73	0.42	0.87	1.07	FeO
S	0.10	-	-	0.06	-	-	0.17	-	-	SO_3
Ti	-	0.12	-	-	0.09	-	-	0.24	-	TiO_2
C	-	-	15.03	-	-	12.41	-	-	34.97	CO_2
O	40.57	43.44	34.83	58.65	61.79	48.99				
							0.94	12.93		H_2O
Total	100.00	100.00	100.00	100.00	100.00	100.00	100.00	100.00	100.00	

Since obsidian is X-ray amorphous, its diffraction pattern is not presented. The diffraction patterns and bargrams of halloysite and dolomite are presented in Figure 1.

Phase identification of the sample revealed that it consists of 69.5 % halloysite, 27.5 % montmorillonite, and 3.00 % quartz. In addition to the main mineral, dolomite, X-ray diffraction analysis also revealed a small amount of quartz.

Journal of Chemistry and Technologies, 2026, *34*(2), 412-424

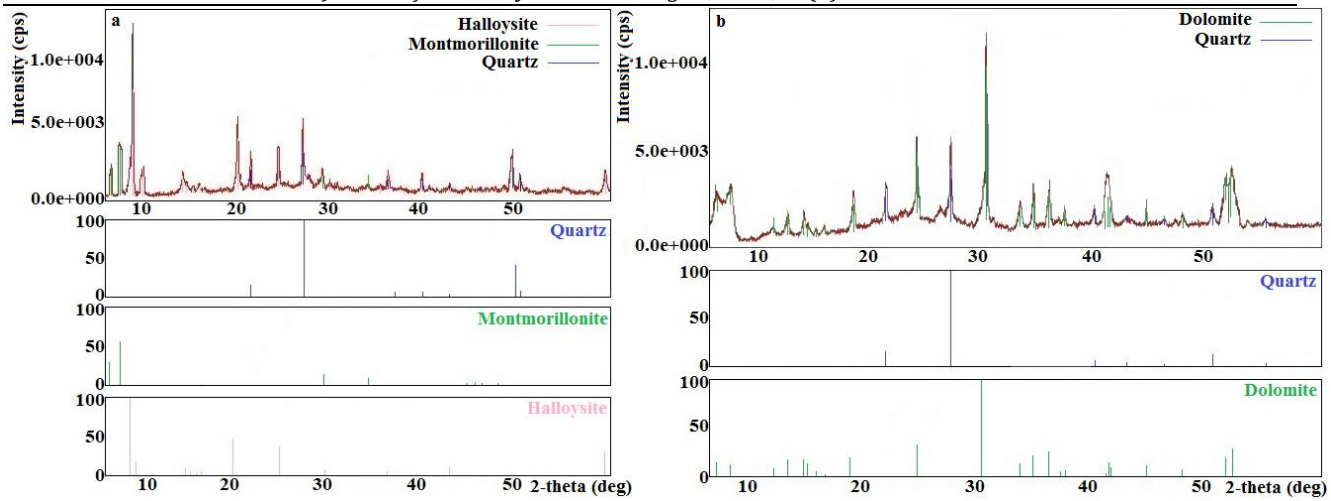

Fig. 1. Diffraction patterns and bargrams of halloysite (a) and dolomite (b)

The crystallization of chabazite-group zeolites based on natural minerals from Nakhchivan was carried out in the presence of a quaternary ammonium hydroxide – tetramethylammonium hydroxide (TMAOH). It should be noted that the use of an organic structure-directing agent facilitates the formation of microporous crystals with varying pore geometries, i.e., the formation of the desired porous structure [26; 27]. Our choice of TMAOH as an organic structure-directing agent significantly influences the crystallization kinetics, as well as the size and morphology of the resulting crystals. On the other hand, the use of organic structure-directing agents facilitates the production of high-silica zeolites, which is important for their thermal stability [28; 29]. High-silica zeolites are also characterized by increased hydrophobicity, which is useful in catalytic reactions.

Diffraction patterns, IR spectra, thermograms, and micrographs of the synthesized zeolites gmelinite, levyne, and erionite are presented in Figures 2–4, respectively.

According to the X-ray phase analysis, the obtained zeolites gmelinite, levyne, and erionite crystallize in the hexagonal crystal system with parameters a = 13.78 Å, c = 10.10 Å; in the rhombohedral crystal system with parameters a = 10.75 Å, α = 76°25'; and in the hexagonal crystal system with parameters a = 13.15 Å, c = 15.05 Å, respectively. The Bragg angles 2θ of the synthesized gmelinite, levyne, and erionite correspond to the values 7.42, 11.52, 17.31, 17.65, 21.63, 30.02, 33.34, 34.52, 39.31° (Fig. 2 (a)); 8.56, 10.85, 11.53, 20.77, 21.77, 31.95, 34.14, 35.62° (Fig. 3 (a)); 7.69, 9.68, 11.76, 13.34, 20.45, 23.65, 24.90, 31.46, 35.81, 36.10° (Fig. 4 (a)), respectively, which are in good agreement with the literature data [30; 31].

Figures 2–4(b) show the IR spectra of gmelinite, levyne, and erionite zeolites, respectively, in the range of 4000–400 cm^{-1}. The absorption bands in the frequency range of 250–1400 cm^{-1} correspond to vibrations of the aluminosilicate tetrahedra of the framework structure of zeolites, that is, to the types of bonds Si–O–Al, Si–O–Si, Si–O, Si–Al [32]. As is known, two types of vibrations are characteristic of zeolites: Type 1 – vibrations characterizing the primary structural units – TO_4, where T represents Si^{4+} or Al^{3+} cations; Type 2 – vibrations of TO_4 tetrahedra along the external bonds [33]. The first type of vibrations includes asymmetric, symmetric, and deformation (bending) vibrations of T–O bonds in the ranges of 1250–950, 720–650, and 500–420 cm^{-1}. The second type of vibrations includes asymmetric and symmetric vibrations of external bonds and vibrations of double chains in the ranges of 1150–1050, 820–750, and 650–500 cm^{-1}. The presence of zeolitic water corresponds to absorption bands in the range of 3100–3700 cm^{-1}, while the region of 1600–1660 cm^{-1} contains bending vibration bands characteristic of molecular water (Si–OH, Si–OH–Al, and –OH).

The bands at 1048, 796, and 693 cm^{-1} for gmelinite, 1050, 781, and 645 cm^{-1} for levyne, and 71049, 78, and 460 cm^{-1} or erionite can be attributed to the asymmetric stretching vibration of the inner tetrahedron, symmetric stretching vibration, and bending vibrations of T–O bonds in TO_4 tetrahedra, respectively. The bands at 459 cm^{-1} for gmelinite and 460 cm^{-1} for levyne and erionite are due to their main structural unit, and the bands at 1649, 2922, 1630, and 1637 cm^{-1} are attributed to bending vibrations of the OH group in adsorbed water. Finally, a typical broad water band is present in the 3000–3500 cm^{-1} region with

Journal of Chemistry and Technologies, 2026, *34*(2), 412-424

an extremum at 3447 cm^{-1} for gmelinite, 3489 cm^{-1} for levyne, and 3433 cm^{-1} for erionite.

According to the results of thermal analysis (Fig. 2–4(c)), the differential thermal analysis (DTA) curve for gmelinite zeolite (Fig. 2(c)) is characterized by one endothermic and one exothermic effect. The endothermic effect is related to the sample dehydration, which involves the hydration shell of Na+ cations with a maximum at 250 °C, at which the mass loss according to the TG curve is 21.5 %. The exothermic effect, detected at a temperature of 700 °C, according to X-ray phase analysis, is related to the destruction of the crystalline structure of gmelinite, with anorthite and quartz being found in the products.

The DTA curve for levyne (Fig. 3(c)) is characterized by two endothermic effects. Dehydration of levyne zeolite occurs in two stages. These stages are accompanied by two endothermic effects over a wide temperature range from 100 to 500 °C. Across all these stages, the weight loss is 17.60 %. The first endothermic effect, with a maximum at 160 °C, is attributed to water molecules located in the cavities of the structure, while the second is due to crystalline water within the levyne structure. Complete dehydration of levyne zeolite finishes at 500 °C. As X-ray diffraction analysis showed, the levyne structure is stable up to 1000 °C. However, raising the temperature above this value (i.e., at 1100 °C) disrupts its structure, and albite and cristobalite appear as crystallization products.

The DTA curve of erionite (Fig. 4(c)) is characterized by three endothermic effects. The first two endothermic effects are related to the dehydration of the sample, which occurs in stages. High-temperature dehydration is related to the hydration shell of Mg^{2+} cations. In the first stage, the hydration shell surrounding Ca^{2+} ions undergoes dehydration (with a maximum at 220 °C), while in the second stage, the hydration shell surrounding Mg^{2+} ions (with a maximum at 415 °C) undergoes dehydration. The mass loss according to the TG curve is 26 %. The third endothermic effect, detected at a high temperature with a maximum at 970 °C, according to X-ray phase analysis, is related to the destruction of the zeolite crystal lattice; anorthite and albite were present in the products.

As can be seen from the micrograph of gmelinite (Fig. 2(d)), it is represented by a faceted morphology of various sizes; levyne (Fig. 3(d)) is represented by a spherical morphology of almost uniform sizes; and erionite (Fig. 4(d)) is represented by a grain-shaped (granular) morphology of almost uniform sizes.

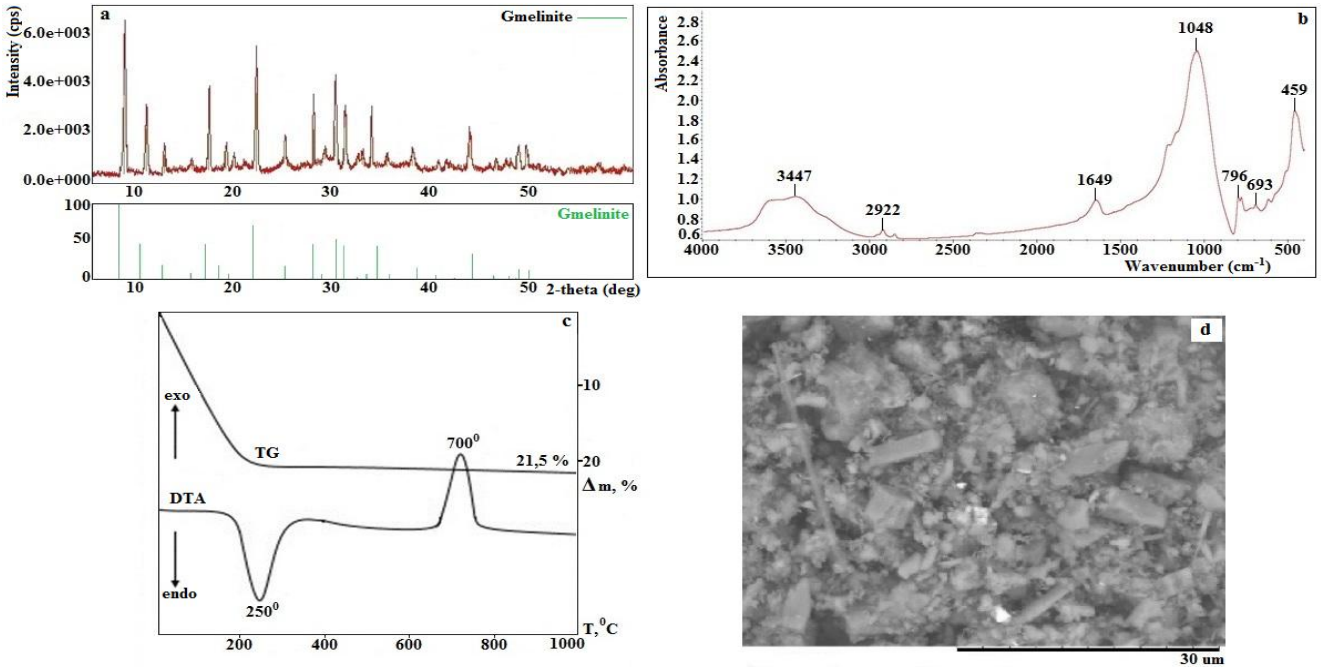

Figure 2. Diffraction pattern (a), IR spectrum (b), thermogram (c) and micrograph (d) of the obtained gmelinite zeolite

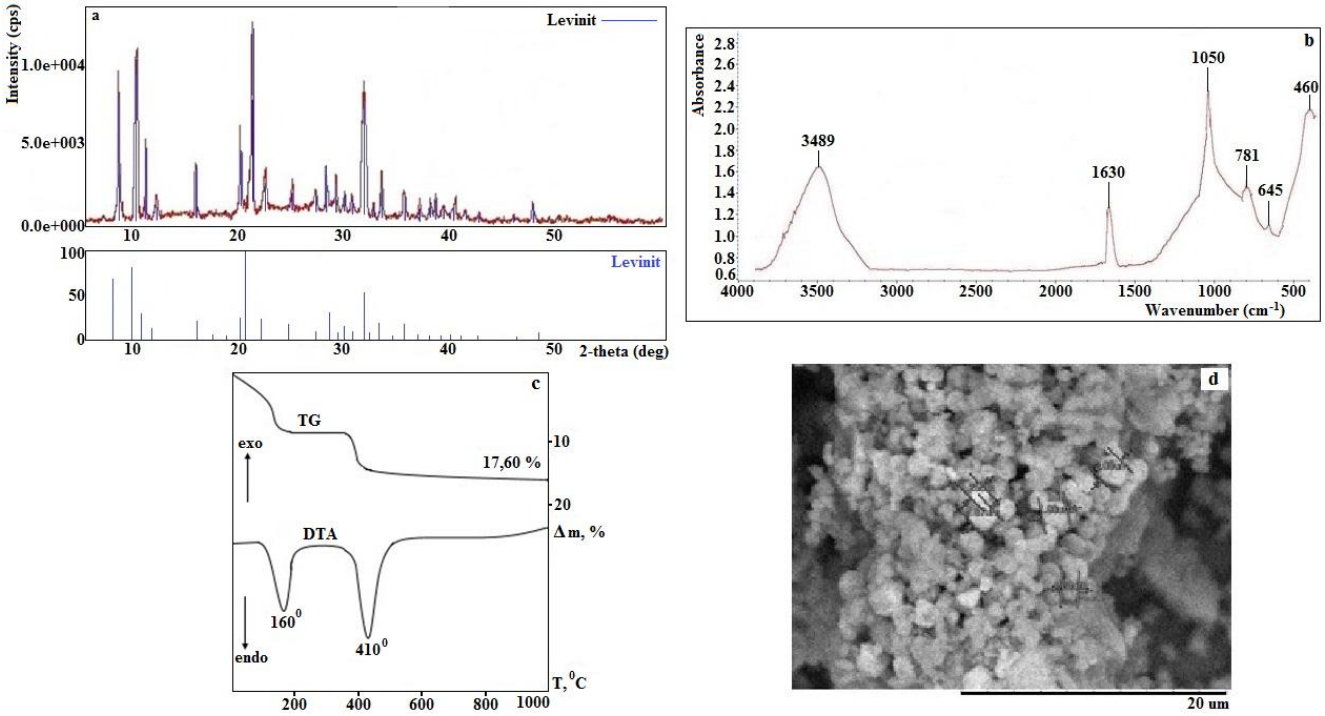

Figure 3. Diffraction pattern (a), IR spectrum (b), thermogram (c) and micrograph (d) of the obtained zeolite levyne

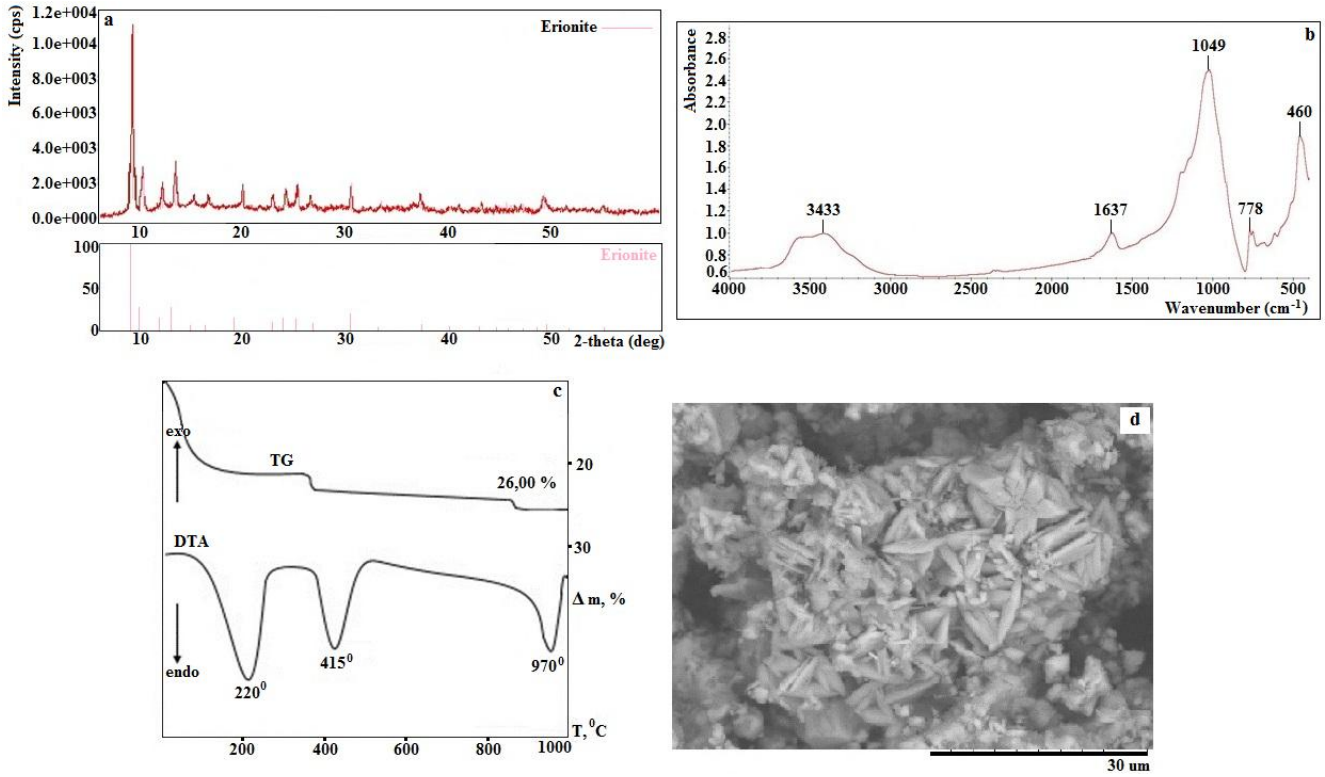

Figure 4. Diffraction pattern (a), IR spectrum (b), thermogram (c) and micrograph (d) of the obtained erionite zeolite

Figure 5 shows diffraction patterns and bargrams of the products of destruction of the structures of gmelinite (a), levyne (b) and erionite (c).

Journal of Chemistry and Technologies, 2026, *34*(2), 412-424

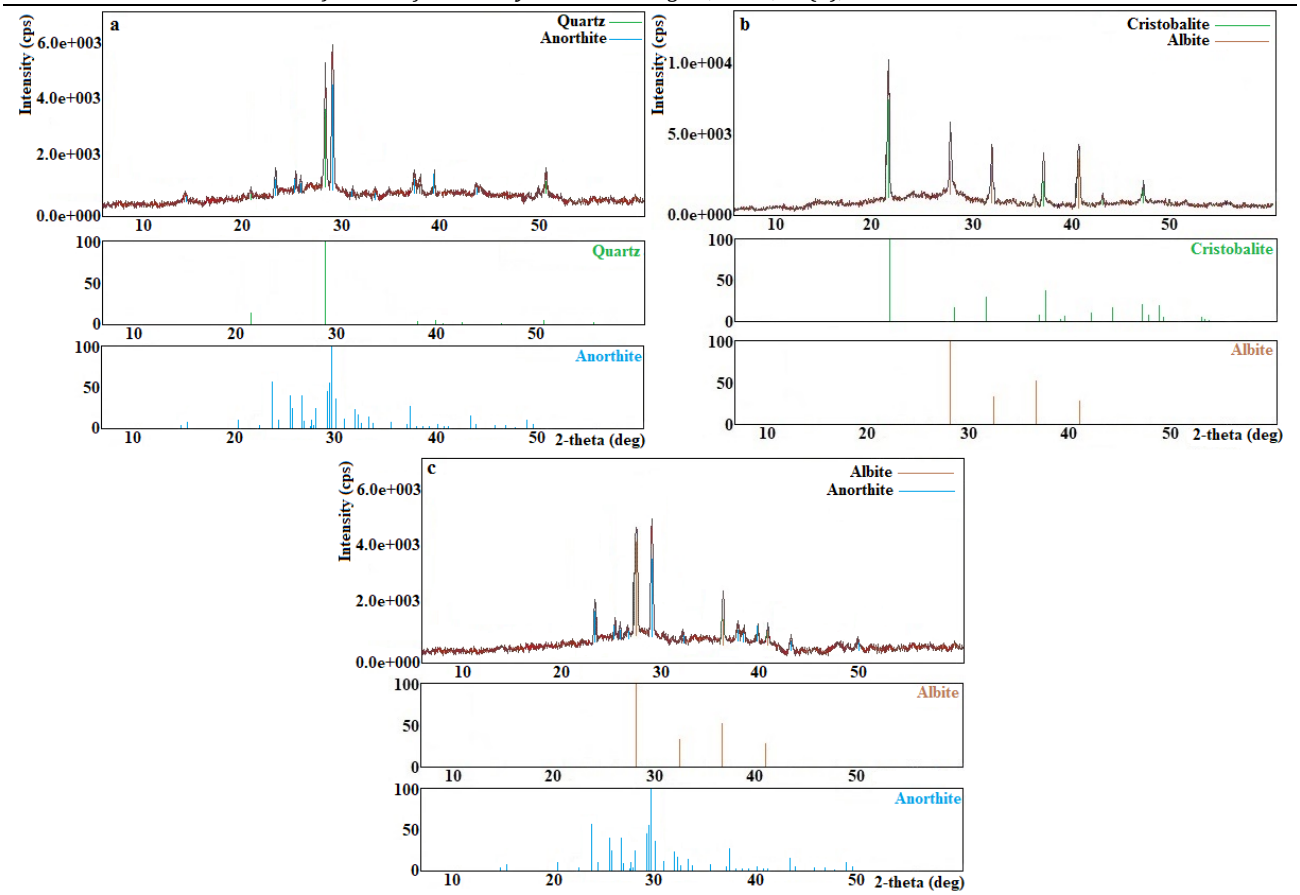

Figure 5. Diffraction patterns and bargrams of the products of destruction of the structures of gmelinite (a), levyne (b), erionite (c)

As mentioned above, experiments on the hydrothermal synthesis of gmelinite, levyne, and erionite were studied in the temperature range of 100–300 °C, with the concentration of the thermal NaOH solution varying in the range of 10–35 % for 50–200 hours; 100–300 °C, with the concentration of the thermal NaOH solution varying in the range of 10–35 % for 50–150 hours; and 100–200 °C, with the concentration of the thermal NaOH solution varying in the range of 10–30 % for 10–20 hours, respectively.

The obtained results allow us to conclude that the optimal conditions for obtaining phase-pure gmelinite, levyne, and erionite zeolites with a 100 % degree of crystallinity were: a temperature of 200 °C, a thermal NaOH solution concentration (C_{NaOH}) of 20–30 %, and a processing time of 100 hours; 200 °C, C_{NaOH} of 20–30 %, and a processing time of 100 hours; and 150 °C, C_{NaOH} of 15–20 %, and a processing time of 12 hours, respectively.

The effects of temperature, thermal solution concentration, and processing time on the crystallization process of erionite, gmelinite, and levyne zeolites were systematically evaluated. The X-ray diffraction (XRD) patterns of the products obtained during the study of erionite crystallization under various conditions are shown in Figure 6.

As shown above, the precise temperature required to obtain phase-pure erionite zeolite with 100 % crystallinity is 150 °C. At temperatures below 150 °C (specifically, in the range of 100–150 °C), the crystallization products contained low-crystalline erionite and cristobalite (Fig. 6(a)). In contrast, in the temperature range of 150–200 °C, phillipsite and analcime crystallized (Fig. 6(b)).

As noted, the optimal region of existence for pure erionite is an alkalinity of 15–20 % NaOH. At a thermal NaOH concentration below 15 % (specifically, in the range of 10–15 %), the products contained low-crystalline erionite, albite, and phillipsite (Fig. 6(c)). Increasing the alkalinity above 20 % (up to 30 %) promotes the formation of a mixture of erionite, phillipsite, chabazite, and albite. More precisely, in the alkalinity range of 20–25 %, the crystallization products contained erionite and phillipsite (Fig. 6(d)), while in the 25–30 % range, phillipsite, chabazite, and albite were detected (Fig. 6(e)).

According to the data presented above, the region of existence of phase-pure erionite with 100 % crystallinity corresponds to a processing

Journal of Chemistry and Technologies, 2026, *34*(2), 412-424

time of 12 hours. The crystallization process was studied in the time range of 10–20 hours. At processing times below 12 hours (i.e., in the 10–12 hour range), according to X-ray phase analysis, crystallization did not begin. Increasing the processing time above 12 hours (up to 20 hours) promotes phillipsite crystallization (Fig. 6(f)).

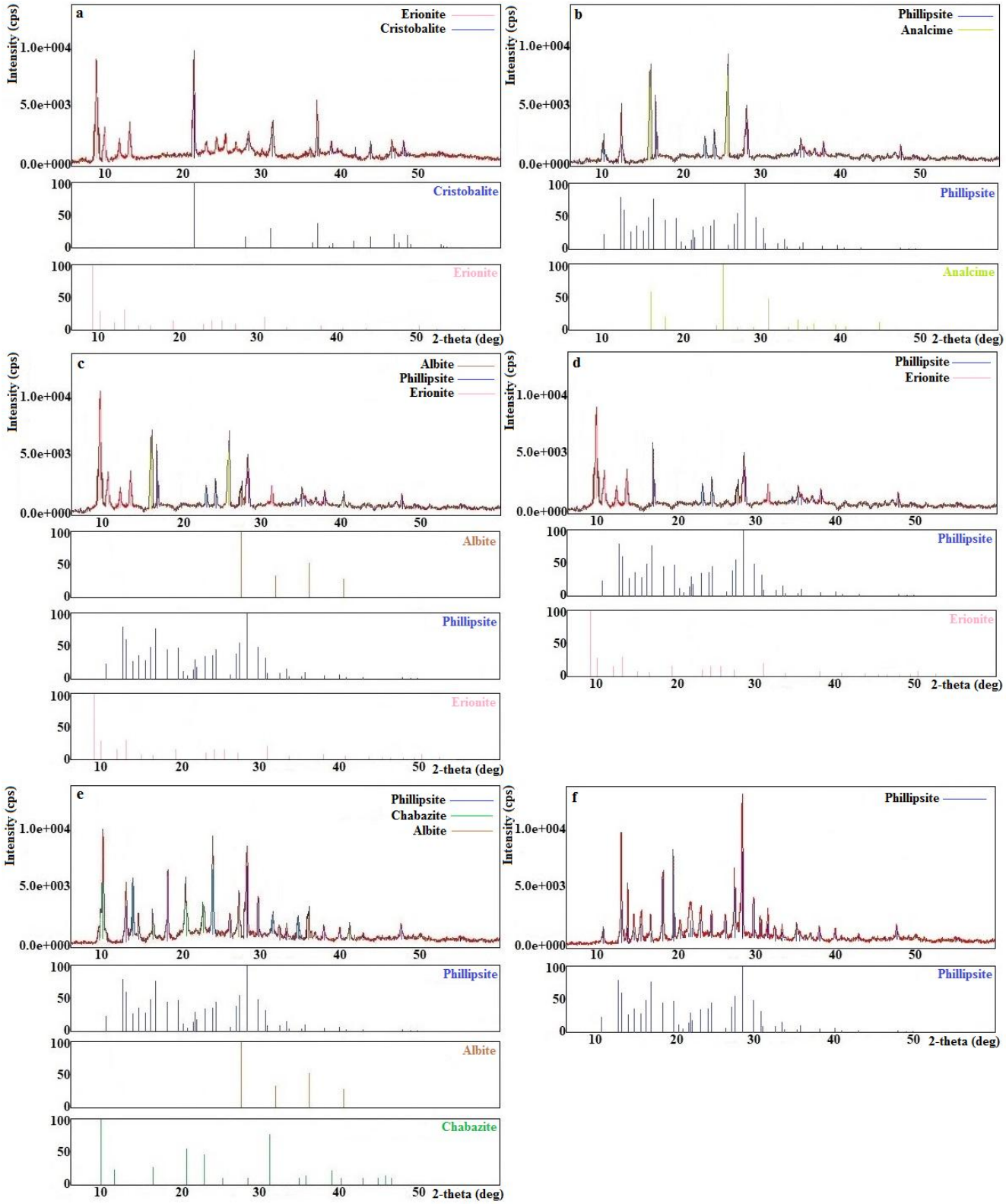

Figure 6. XRD patterns and bargrams of erionite crystallization products: (a) erionite + cristobalite (at a temperature below 150 °C); (b) phillipsite + analcime (at a temperature of 150–200 °C); (c) erionite + albite + phillipsite (at a NaOH concentration of 10–15 %); (d) erionite + phillipsite (at a NaOH concentration of 20–25 %); (e) phillipsite + chabazite + albite (at a NaOH concentration of 25–30 %); (f) phillipsite (at a crystallization time above 12 hours)

The XRD patterns of the products obtained during the study of levyne crystallization under various conditions are shown in Figure 7.

A study of the effect of temperature on the crystallization process of zeolite levyne revealed that changing the optimal conditions leads to the formation of different products. Specifically, a decrease in temperature below 200 °C (down to 100 °C) promoted the formation of phillipsite and chabazite (Fig. 7(a)), while an increase in temperature above the optimal value (up to 300 °C) promoted the formation of a mixture of levyne, phillipsite, and albite (Fig. 7(b)).

As noted above, the optimal region for the existence of phase-pure levyne is a thermal solution concentration of 20–30 %. At a thermal solution concentration below 20 % (specifically, 10–20 %), the crystallization products contained low-crystalline levyne and cristobalite (Fig. 7(c)). Increasing the NaOH concentration above 30 % (up to 35 %) promotes the formation of pure chabazite (Fig. 7(d)).

According to the data presented above, the region of existence of levyne with 100 % crystallinity is a processing time of 100 hours. The crystallization process was studied in the time range of 50–150 hours. At processing times below 100 hours (i.e., in the range of 50–100 hours), according to X-ray phase analysis, the products contained low-crystalline levyne and phillipsite (Fig. 7(e)). In the time range of 100–150 hours, the crystallization products contained levyne and analcime (Fig. 7(f)). Increasing the processing time above 150 hours promotes the crystallization of pure analcime (Fig. 7(g)).

The XRD patterns of the products obtained during the study of the gmelinite synthesis process under various conditions are shown in Figure 8.

In the case of gmelinite, the effect of temperature on the crystallization process revealed that a decrease in temperature below 200 °C (down to 100 °C) facilitated the formation of low-crystalline gmelinite and cristobalite (Fig. 8(a)). Increasing the temperature above the optimum (up to 300 °C) facilitated the formation of a mixture of gmelinite, analcime, and albite (Fig. 8(b)).

As noted above, the optimal region for the existence of phase-pure gmelinite is a thermal solution concentration of 20–30 %. At thermal solution concentrations below 20 % (specifically, 10–20 %), the crystallization products contained low-crystalline zeolite gmelinite, phillipsite, and cristobalite (Fig. 8(c)). Increasing the NaOH concentration above 30 % (up to 35 %) promotes the formation of a mixture of gmelinite and analcime (Fig. 8(d)).

The region of existence of gmelinite with 100% crystallinity corresponds to a processing time of 100 hours. The crystallization process was studied in the time range of 50–200 hours. At processing times below 100 hours (i.e., in the range of 50–100 hours), according to X-ray phase analysis, gmelinite, phillipsite, and cristobalite crystallized (Fig. 8(c)). In the time range of 100–200 hours, phillipsite and analcime were present in the crystallization products (Fig. 8(e)). Increasing the processing time above 200 hours promotes the crystallization of analcime and hydrosodalite (Fig. 8(f)).

Journal of Chemistry and Technologies, 2026, *34*(2), 412-424

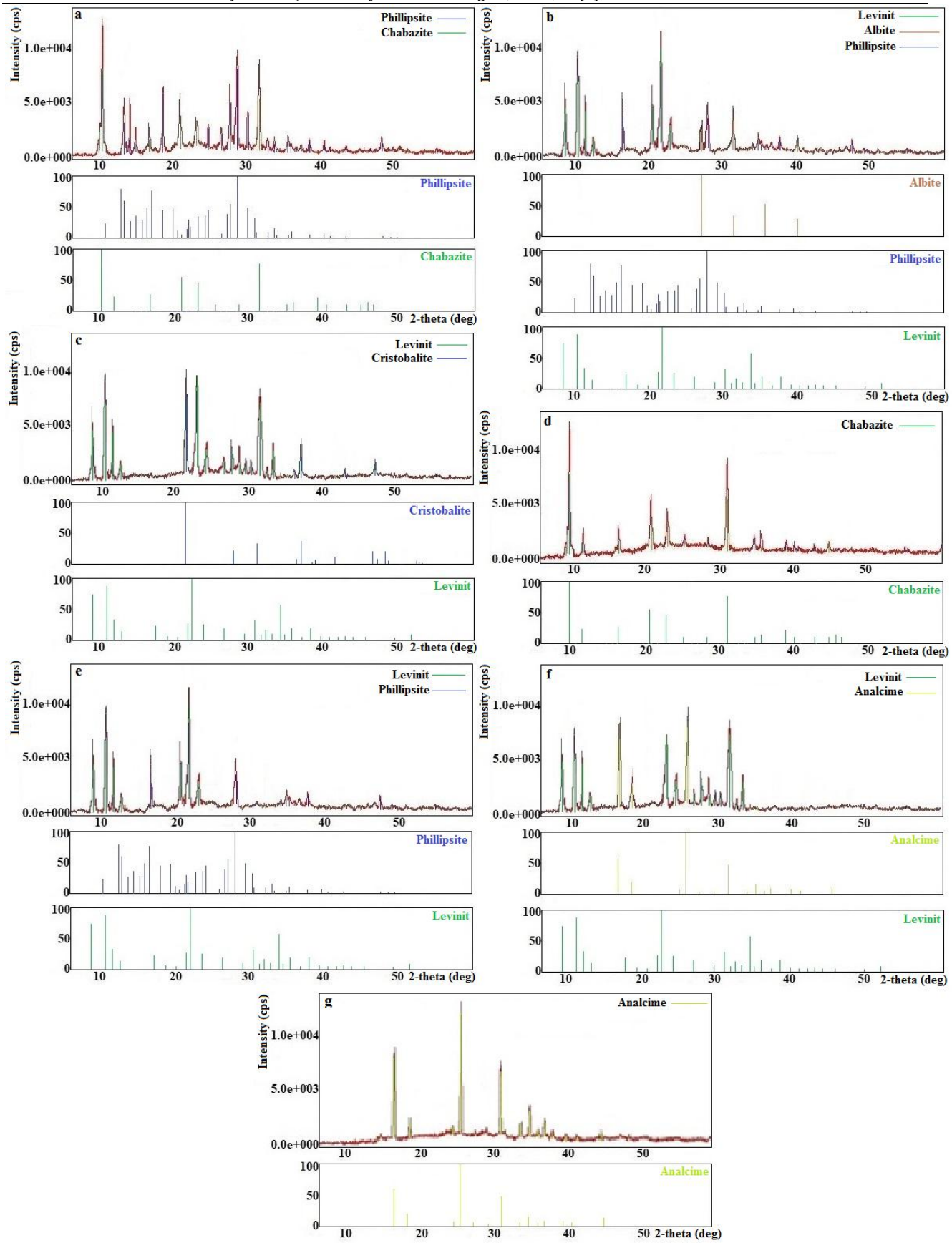

Figure 7. XRD patterns and bargrams of levyne crystallization products: (a) phillipsite + chabazite (at a temperature below 200 °C); (b) phillipsite + levyne + albite (at a temperature of 200–300 °C); (c) levyne + cristobalite (at a NaOH concentration of 10–20%); (d) chabazite (at a NaOH concentration of 30–35%); (e) phillipsite + levyne (at a processing time below 100 hours); (f) levyne + analcime (at a processing time of 100–150 hours); (g) analcime (at a processing time above 150 hours).

Journal of Chemistry and Technologies, 2026, *34*(2), 412-424

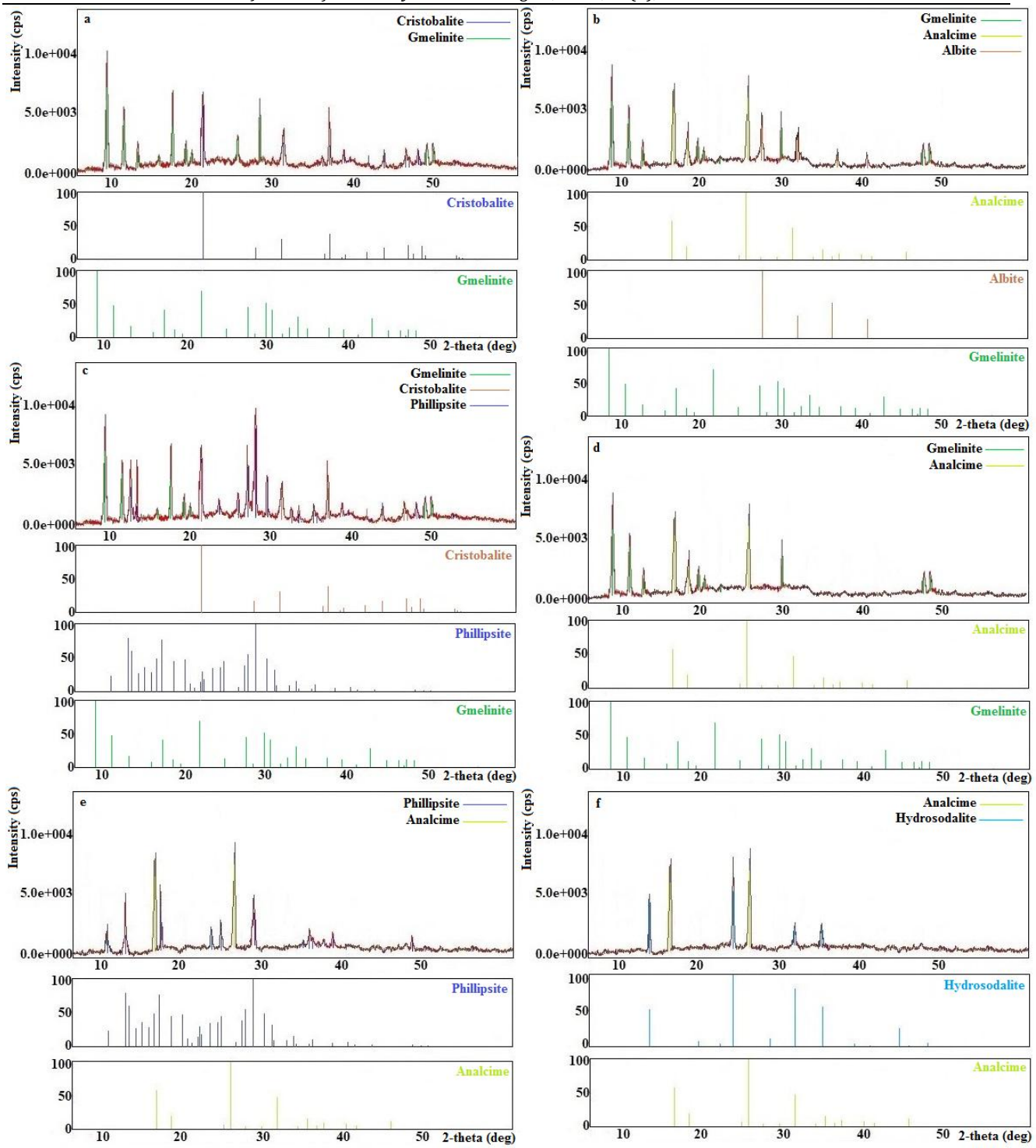

Figure 8. XRD patterns and bargrams of gmelinite crystallization products: (a) gmelinite + cristobalite (at a temperature below 200 °C); (b) gmelinite + analcime + albite (at a temperature of 200–300 °C); (c) gmelinite + phillipsite + cristobalite (at a NaOH concentration below 20% and a crystallization time below 100 hours); (d) gmelinite + analcime (at a NaOH concentration of 30–35%); (e) phillipsite + analcime (at a processing time of 100–200 hours); (f) analcime + hydrosodalite (at a processing time above 200 hours)

Conclusions

Zeolites of practical importance – gmelinite, levyne, and erionite – were synthesized in the presence of TMAOH, using natural minerals from the Nakhchivan Autonomous Republic: obsidian, halloysite, and dolomite.

Experiments on the hydrothermal synthesis of gmelinite, levyne, and erionite were studied in the temperature range of 100–300 °C, with a thermal NaOH solution concentration varying within the range of 10–35 % for 50–200 hours; 100–300 °C, with a thermal NaOH solution concentration varying within the range of 10–35 % for 50–

150 hours; and 100–200 °C, with a thermal NaOH solution concentration varying within the range of 10–30 % for 10–20 hours, respectively.

The optimal ranges of conditions for the synthesis of gmelinite, levyne, and erionite with 100 % crystallinity and phase purity were: temperature 200 °C, concentration of thermal NaOH solution (C_{NaOH}) – 20–3 0%, processing time – 100 hours; 200 °C, C_{NaOH} – 20–30 %, processing time – 100 hours; and 150 °C, C_{NaOH} – 15–20 %, processing time – 12 hours, respectively.

For erionite, it was found that at temperatures below 150 °C, low-crystalline erionite and cristobalite were present in the crystallization products, while above 150 °C, phillipsite and analcime were formed; at a thermal solution concentration below 15 %, low-crystalline erionite, albite, and phillipsite are obtained, while above 20 %, erionite, phillipsite, chabazite, and albite are formed; at a processing time of less than 12 hours, crystallization did not begin, and above 12 hours, phillipsite crystallized.

For levyne, it was found that at temperatures below 200 °C, phillipsite and chabazite were among the crystallization products, while above 200 °C (in the range of 200–300 °C), levyne, phillipsite, and albite were obtained; at a thermal solution concentration below 20 %, low-crystalline levyne and cristobalite are obtained, while above 30 %, pure chabazite is obtained; at a processing time of less than 100 hours, low-crystalline levyne and phillipsite are obtained, in the range of 100–150 hours, levyne and analcime were obtained, and above 150 hours, pure analcime crystallized.

For gmelinite, it was found that at temperatures below 200 °C, the crystallization products included low-crystalline gmelinite and cristobalite, while at temperatures above 200 °C, they included gmelinite, albite, and analcime. At thermal solution concentrations below 20 %, low-crystalline gmelinite, phillipsite, and cristobalite were obtained, while above 30 %, gmelinite and analcime were formed. Processing times below 100 hours produced gmelinite, phillipsite, and cristobalite; between 100 and 200 hours, phillipsite and analcime were obtained; and above 200 hours, analcime and hydrosodalite crystallized.

References

[1] Jihong, Y. (2007). Chapter 3 – synthesis of zeolites. *Studies in Surface Science and Catalysis*, *168*, 39-103. https://doi.org/10.1016/S0167-2991(07)80791-9

[2] Mgbemere, H. E., Ekpe, I. C., Lawal, G. (2017). Zeolite synthesis, characterization and application areas: a review. *International Research Journal of Environmental Science*, *10*, 45–59. https://ir.unilag.edu.ng/handle/123456789/10226

[3] Moshoeshoe, M., Nadiye-Tabbiruka, M. S., Obuseng, V. (2017). A review of the chemistry, structure, properties and applications of zeolites. *American Journal of Materials Science*, *7*, 196–221. https://doi.org/10.5923/j.materials.20170705.12

[4] Mielby, J., Hauberg, K., Iltsiou, D., Goodarzi, F., Enemark-Rasmussen, K., Kegnaes, S. (2022). A shortcut to high-quality gmelinite through steam-assisted interzeolite transformation. *Microporous and Mesoporous Materials*, *330*, 111606. https://doi.org/10.1016/j.micromeso.2021.111606

[5] Alberti, A., Parodi, I., Cruciani, G., Dalconi, M. C., Martucci, A. (2010). Dehydration and rehydration processes in gmelinite: An in situ X-ray single-crystal study. *American Mineralogist*, *95*(11-12), 1773–1782. https://doi.org/10.2138/am.2010.3419

[6] Dusselier, M., Kang, J. H., Xie, D., Davis, M. E. (2017). CIT-9: a fault-free gmelinite zeolite. *Angewandte Chemie International Edition*, *56*(43), 13475-13478. https://doi.org/10.1002/anie.201707452

[7] Xie, D., Lacheen, H. S. (2016). Separation of Gases Using GME Framework Type Zeolites. US Patent 9364782.

[8] Parsons, D. S., Ingram, A., Hriljac, J. A. (2023). The synthesis of gmelinite microspheres and their post-synthetic modification for improved defluoridation. *Separation Science and Technology*, *58*(10), 1851–1862. https://doi.org/10.1080/01496395.2023.2212853

[9] Chatterjee, M., Ganguli, D., Saha, P. (2014). Synthesis and characterization of gmelinite- and chabazite-type molecular sieve zeolites. *Transactions of the Indian Ceramic Society*, *35*(5), 99–105. https://doi.org/10.1080/0371750X.1976.10840871

[10] Chiyoda, O., Davis, M. E. (2000). Adsorption studies with gmelinite zeolites containing mono-, di- and trivalent cations. *Microporous and Mesoporous Materials*, *38*(2–3), 143-149. https://doi.org/DOI:10.1016/S1387-1811(99)00287-5

[11] Arletti, R., Vezzalini, G., Quartieri, S., et al. (2013). A new framework topology in the dehydrated form of zeolite levyne. *American Mineralogist*, *98*(11-12), 2063–2074. https://doi.org/10.2138/am.2013.4583

[12] Ballirano, P., Cametti, G. (2013). Crystal chemical and structural investigation of levyne-Na. *Mineralogical Magazine*, *77*(7), 2887–2899. https://doi.org/10.1180/minmag.2013.077.7.01

[13] Cametti, G., Scheinost, A., Churakov, S. (2021). Cd2+ incorporation in small-pore LEV/ERI intergrown zeolites: A multi-methodological study. *Microporous and Mesoporous Materials*, *313*, 110835. https://doi.org/10.1016/j.micromeso.2020.110835

[14] Al Atrach, J., Aitblal, A., Amedlous, A., et al. (2025). Exploring a novel adsorbent for CO2 capture and gas separation. *ACS Applied Materials & Interfaces*, *17*(4), 7119–7130. https://doi.org/10.1021/acsami.4c18745

[15] Min, J. G., Kemp, K. C., Hong, S. B. (2020). Propylene/propane separation on a ferroaluminosilicate levyne zeolite. *Microporous and Mesoporous Materials*, *294*, 109833. https://doi.org/10.1016/j.micromeso.2019.109833

[16] Venkatathri, N., Yoo, J. W. (2008). Synthesis, characterization and catalytic properties of a LEV type

silicoaluminophosphate molecular sieve, SAPO-35 from aqueous media using aluminium isopropoxide and hexamethyleneimine template. *Applied Catalysis A: General*, *340*(2), 265–270. https://doi.org/10.1016/j.apcata.2008.02.026

[17] Jeon, H. Y., Shin, C. H., Jung, H. J., et al. (2006). Catalytic evaluation of small-pore molecular sieves with different framework topologies for the synthesis of methylamines. *Applied Catalysis A: General*, *305*(1), 70-78. https://doi.org/10.1016/j.apcata.2006.02.044

[18] Mgbemere, H. E., Ekpe, I. C. (2017). Zeolite synthesis, characterization and application areas: a review. *International Journal of Environmental Science*, *6*(10), 45–59. https://ir.unilag.edu.ng/handle/123456789/10226

[19] Lee, J. H., Park, M. B., Lee, J. K., Min, H. K., Song, M. K., Hong, S. B. (2010). Synthesis and characterization of ERI-type UZM-12 zeolites and their methanol-to-olefin performance. *Journal of the American Chemical Society*, *132*(37), 12971–12982. https://doi.org/10.1021/ja105185r

[20] Seo, S., Ahn, N. H., Lee, J. H., Knight, L. M., Moscoso, J. G., Sinkler, W. A., Prabhakar, S., Nicholas, C. P., Hong, S. B., Lewis, G. J. (2019). Combined alkali-organoammonium structure direction of high-charge-density heteroatom-containing aluminophosphate molecular sieves. *Angewandte Chemie International Edition*, *58*(27), 9032–9037. https://doi.org/10.1002/anie.201902623

[21] Passaglia, E., Artioli, G., Gualtieri, A. (1998). Crystal chemistry of the zeolites erionite and offretite. *American Mineralogist*, *83*, 577-589. DOI:10.2138/am-1998-5-618

[22] Zhu, J., Muraoka, K., Ohnishi, T., Yanaba, Y., Ogura, M., Nakayama, A., Wakihara, T., Liu, Z., Okubo, T. (2024). Synthesis and structural analysis of high-silica ERI zeolite with spatially-biased Al distribution as a promising NH3-SCR catalyst. *Advanced Science*, *11*(14), 2307674. https://doi.org/10.1002/advs.202307674

[23] Khanday, W. A., Khanday, S. A., Danish, M. (2020). Application of erionite as an adsorbent for Cd2+, Cu2+, and Pb2+ ions in water. *Desalination and Water Treatment*, *205*, 328–335. https://doi.org/10.5004/dwt.2020.26309

[24] Rayalu, S., Udhoji, J., Meshram, S., Naidu, R., Devotta, S. (2005). Estimation of crystallinity in flyash-based zeolite-A using XRD and IR spectroscopy. *Current Science*, *89*(12), 2147.

[25] Ayoola, A. A., Hymore, F. K., Omodara, J. O., Oyeniyi, A. E., Ojo, S. F., Chisom, U. (2017). Effect of crystallization time on the synthesis of zeolite Y from Elefun kaolinite clay. *International Journal of Applied Engineering Research*, *12*(21), 10981.

[26] Simancas, R., Dari, D., Navarro, M. T., Velamazan, N. (2010). Modular organic structure-directing agents for the synthesis of zeolites. *Science*, *330*(6008), 1219. https://doi.org/10.1126/science.1196240

[27] Oleksiak, M. D., Rimer, J. D. (2014). Synthesis of zeolites in the absence of organic structure-directing agents: factors governing crystal selection and polymorphism. *Reviews in Chemical Engineering*, *30*(1), 1. https://doi.org/10.1515/revce-2013-0020

[28] Burton, A. W., Zones, S. I. (2007). Chapter 5 Organic molecules in zeolite synthesis: their preparation and structure-directing effects. *Studies in Surface Science and Catalysis*, *168*, 137. https://doi.org/10.1016/S0167-2991(07)80793-2

[29] Pour, Z. A., Sebakhy, Kh. O. (2022). A review on the effects of organic structure-directing agents on the hydrothermal synthesis and physicochemical properties of zeolites. *Chemistry*, *4*(2), 431. https://doi.org/10.3390/chemistry4020032

[30] Treacy, M. M. J., Higgins, J. B. (2001). Collection of simulated XRD powder patterns for zeolites. Elsevier.

[31] Baerlocher, C., McCusker, L. B., Olson, D. H. (2007). *Atlas of zeolite framework types* (6th ed.). Elsevier Inc.

[32] Byrappa, K., Suresh Kumar, B. V. (2007). Characterization of zeolites by infrared spectroscopy. *Asian Journal of Chemistry*, *19*(6), 4933–4935.

[33] Krol, M., Mozgawa, W., Jastrzbski, W., Barczyk, K. (2012). Application of IR spectra in the studies of zeolites from D4R and D6R structural groups. *Microporous and Mesoporous Materials*, *156*, 181–188. https://doi.org/10.1016/j.micromeso.2012.02.040